Published in final edited form as:
Invest Radiol. 2009 September ; 44(9): 619–626. doi:10.1097/RLI.0b013e3181b4c218.

Three-dimensional T2-weighted MRI of the Human Femoral Arterial Vessel Wall at 3.0Tesla

Zhuoli Zhang[1], **Zhaoyang Fan**[1,2], **Timothy J. Carroll**[1,2], **YiuCho Chung**[3], **Peter Weale**[3], **Renate Jerecic**[3], and **Debiao Li**[1,2]

[1]Department of Radiology, Northwestern University, Chicago, Illinois, United States

[2]Department of Biomedical Engineering, Northwestern University, Evanston, Illinois, United States

[3]Siemens Medical Solutions, Chicago, Illinois, United States

Abstract

OBJECTIVES—To evaluate the potential use of a novel 3D turbo spin-echo (TSE) T2-weighted (T2w) technique for assessing the vessel wall in the superficial femoral artery at 3.0T.

BACKGROUND—Magnetic resonance imaging (MRI) can be used for the noninvasive assessment of atherosclerotic plaque burden in the peripheral circulation. While black-blood 2D TSE techniques have been used for femoral arterial wall imaging, these techniques require prolonged imaging time to cover a large field of view required to cover the leg. Recently, variable-flip-angle 3D TSE T2w (SPACE) has been introduced as a fast vessel wall imaging technique with submillimeter spatial resolution. A systematic investigation of the application of this technique to femoral arterial wall imaging has yet to be performed.

METHODS—Fifteen healthy volunteers and 3 patients with peripheral arterial disease (PAD) underwent 3D SPACE imaging of the superficial femoral artery at 3.0T, with the conventional 2D TSE T2w imaging as a reference. Muscle-lumen contrast to noise ratio (CNR) and wall/lumen volumes (WV, LV) were measured at the matched locations on the 3D and 2D image sets. Statistical comparison on a per-subject basis was conducted to determine the difference and agreement between 3D SPACE and the 2D TSE techniques.

RESULTS—The 3D SPACE data sets enabled vessel visualization from arbitrary orientation through multi-planar reformation (MPR) technique. Muscle-lumen CNR was significantly higher with 3D SPACE than with the 2D TSE (3.12 ± 0.84 vs. 2.17 ± 0.34, $p < 0.01$). This trend was confirmed when CNR efficiency (CNR_{eff}) values were further compared. A similar trend was observed in PAD patients (SPACE vs. 2D TSE T2w: CNR 2.35 ± 0.13 vs. 1.77 ± 0.25; CNR_{eff} 15.35 ± 0.61 vs. 3.59 ± 2.62. all $p < 0.05$). Measurements of WV and LV from the 3D and 2D techniques were highly correlated in volunteers and PAD patients (volunteers, WV: linear regression $r^2 = 0.98$, LV: $r^2 = 0.98$, $p < 0.001$ for both; patients, WV: linear regression $r^2 = 0.96$, LV: $r^2 = 0.94$, $p < 0.001$ for both).

CONCLUSION—We established the feasibily of using the 3D SPACE technique for vessel wall imaging in the superficial femoral artery at 3.0T. High-, isotropic-resolution SPACE images, with the aid of MPR, enable superior vessel wall visualization. Superior blood signal suppression comparable vessel wall vessel wall morphological measurements, and superior time efficiency relative to conventional 2D TSE imaging suggest the great potential of the SPACE method as a non-invasive imaging technique for the assessment of atherosclerotic plaque burden in PAD patients.

Corresponding Author: Debiao Li Northwestern University Department of Radiology 737 N Michigan Ave; Suite 1600 Chicago, Illinois 60611 Phone: (312) 926 - 4245 Fax: (312) 896 - 5665 d-li2@northwestern.edu.

Keywords

MRI; Superficial femoral artery; Vessel wall; 3D TSE

INTRODUCTION

Peripheral arterial disease (PAD) currently affects 8–12 million Americans and by the year 2050 it is expected to reach a prevalence of 19 million Americans [1]. Although ankle–brachial index (ABI) is an excellent test for identifying peripheral arterial obstruction and is sufficient to diagnose PAD in a large percentage of patients [2,3,4], the ABI is limited in its utility for assessing disease severity and therapy [5]. Intravascular ultrasound (IVUS) is currently the diagnostic standard for the quantification of coronary vessel wall plaque [6,7], but it is expensive, invasive and poorly suited for the peripheral circulation. Thus, there is an urgent need to have non-invasive approaches for directly evaluating disease in the arterial wall, quantifying the disease burden and potentially the response to therapy.

Magnetic resonance imaging (MRI) has emerged as a noninvasive imaging modality for assessing vascular disease. Of the various techniques, MR angiography (MRA) techniques are used to evaluate vessel stenosis or occlusion by imaging the vessel lumen rather than vessel wall. In contrast, black-blood vessel wall imaging directly visualizes the vessel wall and may provide complimentary information regarding plaque components and vulnerability [8]. The size, shape, or composition of the arterial wall can be studied by the acquisition of high-resolution, multi-contrast axial images [9,10]. While MRI has been employed for measuring vessel wall and vascular lesions in coronary and carotid arteries, and aorta [7–10], few studies have investigated its role in peripheral circulation [11,12].

MRI has been used for the noninvasive assessment of vessel wall and atherosclerotic plaque burden in the peripheral circulation with two dimensional (2D) “black blood” (BB) turbo spin-echo (TSE) techniques for femoral arterial wall and plaque imaging [11]. However the need for large fields of view, high spatial resolution in the slice-select direction and limited signal-to-noise ratio (SNR) indicate the need for the development of three dimensional (3D) plaque imaging pulse sequences and protocols. We have developed an imaging protocol, based on the 3DSPACE sequence, to address some of the shortcomings of currently available 2D imaging protocols. We report on our assessment of a black-blood 3D pulse sequence optimized for vessel wall imaging of the SFA.

MATERIALS AND METHODS

Study Population

Included in the study were 15 healthy volunteers (twelve men, three women; age range 23–41 years); all volunteers who were recruited had no history of PAD. Three PAD patients (two men, one women; age 69, 72, 78 years) were recruited. All patients had symptoms of intermittent claudication without critical limb ischemia and an ankle-brachial index (ABI: 0.5, 0.6, 0.8) were eligible for this study. The study was performed in compliance with the guidelines of our Institutional Review Board. Written informed consent was obtained from all subjects before MRI was performed.

MR Imaging System and 3D SPACE Imaging Sequence

The study was performed using a clinical 3.0T whole-body MR-system (Siemens Magnetom Trio, Erlangen, Germany). The system was capable of operating at a maximum slew rate of

200 mT/m/ms and a maximum gradient strength of 40 mT/m. The 6 channel body matrix coil anterior and spine coils posterior were used in this work.

The novel 3D SPACE technique employs variable low-flip-angle refocusing RF pulses and achieves lower power deposition and a longer echo train with sufficient signal levels that favors fast imaging [13,14,15,16].

MRI protocol

All subjects were placed supine, and feet first in MR scanner with the thigh at the center of the magnet. The protocol included a multi-planar localizer and a two-dimensional (2D) time-of-flight (TOF) sequence to aid in the localization of the superficial femoral artery.

SPACE was then performed to acquire 3D images of both legs. The scan volume was chosen to include both right and left femoral bifurcations (into superficial and deep femoral arteries) and covered the entire length of the SFAs. SPACE imaging parameters were as follows: TR/TE = 1600/173 ms, number of averages = 2, oblique coronal acquisition with readout in the superior-inferior direction, number of slices = 72, FOV = 380 × 374 mm^2, resolution 0.72 × 0. 72 × 0.72 mm^3, turbo factor = 83, spectrally selective fat saturation, parallel imaging (GRAPPA) acceleration factor = 2, acquisition time (TA) = 11.32 min. A longitudinal coverage of 380 cm was employed in SPACE imaging in order to cover the femoral artery bifurcation and major portion of superficial femoral artery, where atherosclerotic lesions in PAD patients most commonly occur at these locations.

Multi-slice BB 2D TSE T2w imaging with inflow/outflow saturation bands was conducted with 7 axial slices (3 mm thickness, 100% interslice gap) per scan and 2 interleaved scans per segment. A total of 5 segments (10 scans), starting from the femoral artery bifurcation, covered 210-mm-long course of SFA [11]. TR/TE = 2500/57 ms, image resolution = 0.50 × 0.50 × 3 mm^3, FOV = 380 × 370 mm^2, number of average = 2, flip angle = 180°, BW = 338 Hz/pixel, spectrally selective fat saturation, TA per scan = 2 min (4 min per segment). ECG gating was not used according to the previous work [17]. For the volunteer study, 5 segments were acquired. For patients, 2 segments were acquired.

Image Analysis

For the SPACE examinations, Muti-Planar Reformations (MPR) of the SFAs were reconstructed in three directions, using a post-processing workstation (Leonardo, Siemens Medical Solutions).

Landmarks such as characteristic side branches were used for analysis of exact matching vessel segments on 2D TSE and SPACE MPR created cross-section slices with 3 mm thickness.

The 2D cross-section images of SFA were reconstructed from 3D data by MPR. Each pair of 2D cross-section slices of SPACE and 2D multi-slice TSE at the same location were transferred to an imaging workstation with public-domain image processing software (Image J, version 1.37v, National Institutes of Health, Bethesda, MD. USA) for quantitative analysis.

Image Signal Analysis—The evaluation of CNR between the SFA lumen and the muscle was used to characterize the quality of black blood signal suppression. The measurement of SNR and CNR were performed by two experienced observers. Due to the inhomogeneous noise distribution as a result of parallel imaging, we could not directly measure the noise simply in the air. Instead, we used the standard deviation (SD) of the vastus medialis muscle signals enclosed within manually-drawn regions of interests (ROI) greater than 25 mm^2 as the noise, σ_N[18]. Figure 1 shows two matched two axial cross-sectional images of left SFA in 34-year-old woman, left one is 2D TSE image T2w, right one is the same location slice for a 2D time

of flight (TOF) scout image. Arrows point to the SFA in these two images, longer arrows point to deep femoral artery. Note the consistency in size and location of the two arteries (SFA and deep femoral arteries) in the TOF and 2D TSE T2W image. Note the similarity in size and shape of the SFA and deep femoral artery on both images. Vastus medialis muscle (VM) is depicted, and shows where ROI is on the muscle for the measurement of σ_N (figure 1).

The VM signal intensity (S_M) was measured as the average value of 25 mm^2 ROI, while arterial lumen signal intensity (S_L) was measured as the mean signal contained within an ROI drawn to cover the entire lumen. SNR for lumen or muscle were calculated as:

$$\mathrm{SNR}=\mathrm{S}/\sigma_{\mathrm{N}} \tag{1}$$

Where S is the signal intensity, σ_N is the SD of noise. CNR between the lumen and the muscle (CNR_{ML}) was calculated:

$$\mathrm{CNR_{ML}}=\mathrm{SNR_M}-\mathrm{SNR_L} \tag{2}$$

Where SNR_M is the SNR of the muscle, SNR_L is the SNR of the lumen. CNR values were averaged over the measurements from two observers to yield one CNR value for each imaging sequence in each of volunteers. To allow for fair comparison of CNR values with respect to imaging parameter differences, including imaging time, number of slices, and voxel volume, CNR efficiency (CNR_{eff}) was calculated by the relation, adapted from reference [19]:

$$CNR_{eff}=\frac{CNR\sqrt{N}}{VOXEL\sqrt{TA}}=\frac{CNR}{VOXEL\sqrt{TA}_{SLICE}} \tag{3}$$

Where N is the number of imaging slices, TA is the total imaging time, VOXEL is the imaging voxel volume and was expressed in cubic millimeters, TA_{SLICE} is the scan time for each slice (expressed in minutes), and was calculated by dividing total scan time by slice number.

SFA Wall and Lumen Volume Measurements—For volunteers, both 2D TSE images (n = 105) and the 2D MPR cross-sectional images (n = 105) reconstructed from 3D SPACE data, which are the same number (n = 7) of locations for each artery in each volunteer (7 slices were used in each patient), were traced by two experienced observers. The observers were blinded to each other's results. For each individual slice, both lumen and outer contour borders were manually delineated using ImageJ software and the vessel wall area (WA) was measured by subtracting the lumen area (LA) from the outer contour area. The vessel WV (mm^3) and LV (mm^3) in all slices of per volunteer were calculated according to reference [20]:

$$\mathrm{WV}=\mathrm{WA}\times\mathrm{T_{SLICE}} \tag{4}$$

$$\mathrm{LV}=\mathrm{LA}\times\mathrm{T_{SLICE}} \tag{5}$$

Where, T_{SLICE} is individual slice thickness (3 mm).

Statistical Analysis

The 2D TSE T2w images and 2D images reconstructed from SPACE data sets were compared. In each subject, one segment with 7 contiguous image slices from left leg was used for analysis. Statistical comparison included: CNR_{ML} and CNR_{eff} between 2D TSE and SPACE images (signal analysis); lumen volume (LV) and vessel wall volume (WV) between SPACE and TSE images (morphological analysis).

Statistical analysis was performed using Microsoft Excel (Microsoft Corporation, Redmond, WA). Two-tailed paired Student's t-tests were conducted to compare mean values of CNR_{ML} and CNR_{eff}, respectively. Agreement in WV and LV measurements between SPACE and 2D TSE was assessed by linear regression analysis and the method of Bland and Altman. In all tests, statistical significance was defined at the $P < 0.05$ level.

RESULTS

Representative images demonstrating the co-registration at the level of the femoral bifurcation are shown in figure 2. In these images, acquired in a healthy 34-year-old male subject, panel A is curved MPR (slice thickness = 3 mm) from SPACE data set demonstrating that demonstrates the femoral bifurcation (into superficial and deep femoral arteries) with very clear vessel wall and lumen delineation. The common femoral artery and SFA are marked with an “f” and an “s” respectively; where “d” is deep femoral artery. Panel B is four slices of 2D TSE T2w axial images acquired at the level of the four lines demarked in panel A. These cuts correspond to: the common femoral artery, the proximal edge of the bifurcation, mid-bifurcation and SFA/deep femoral artery sections of the vessel respectively. Panel C shows the corresponding 2D slices created from the SPACE volume. The suppression of intra-luminal blood signal was observed with both sequences images of the femoral bifurcation.

Representative images of the SFA obtained with SPACE and 2D TSE in a 32 year old male volunteer are shown in figure 3. Curved MPR image shows the longitudinal view of SFA acquired using SPACE on panel A. Panel B (left) shows 7 axial slices of 2D TSE images of SFA from the plane marked on panel A, Panel B (right), the pairs of SPACE cross-sectional images of the arterial wall created by MPR. Delineation of the SFA wall with suppression of intra-luminal blood signal was observed with both imaging sequences. Imaging time was 11.32 minutes with 38 cm coverage of bilateral SFAs. Representative contiguous images of the femoral artery from a patient with PAD are shown in figure 4. The PAD patient was male and 72 years old with ABI 0.6. MPR of SPACE data shows a longitudinal view of SFA with extensive plaques in panel A, cross-sectional MPR image with 3mm slice thickness of SPACE images on top in panel B (from orientation marked in panel A). On the bottom of panel B is the corresponding 2D TSE T2w image, respectively. Each of these cross-section images shows the atherosclerotic plaques (arrow).

Imaging signal measurements

Quantitative measurements of SFA muscle-lumen CNR and CNR_{eff} values with statistically significant results: Muscle-lumen CNR was significantly higher with 3D SPACE when compared to the reference standard: 2D TSE (SPACE vs. 2D TSE: 3.12 ± 0.84 vs. 2.17 ± 0.34, respectively, $p < 0.01$). This trend was confirmed when CNR_{eff} values were compared. We found the 3D SPACE images to have significantly higher CNR_{eff} (20.75 ± 5.67 vs. 4.01 ± 0.75, respectively, $p < 0.01$). SPACE vs. 2D TSE T2w in PAD patients: CNR 2.35 ± 0.13 vs. 1.77 ± 0.25; CNR_{eff} 15.35 ± 0.61 vs. 3.59 ± 2.62, all $p < 0.05$. By visual inspection, SPACE produced effective suppression of intraluminal flow signal than observed with 2D TSE (see figure 2, 3, 4).

Morphological measurements

Morphological measurements of SFA WV and LV in volunteers made from SPACE and 2D T2w TSE images were highly correlated (WV: linear regression $r^2 = 0.98$, LV: $r^2 = 0.98$, $p < 0.001$ for both). Scatter and Bland-Altman plots for WV and LV are shown in figure 5. Bland-Altman analysis showed good agreement between the data obtained with SPACE and data obtained with 2D T2w TSE. Measured WV and LV values from the SPACE images were, on average, 2.13% and 3.27% smaller than those from 2D TSE after normalization by the average measurements. Bias was not present between measurements of WV ($r = 0.141$; $p > 0.05$) and LV ($r = 0.190$; $p > 0.05$). The measurements of WV and LV from the 3D and 2D techniques were highly correlated in PAD patients, WV: linear regression $r^2 = 0.96$, LV: $r^2 = 0.94$, $p < 0.001$ for both.

Imaging acquisition time comparison between SPACE and 2D TSE techniques

SPACE imaging time was 11. 23 minutes to cover 38-cm-long course of SFA. 2D multislice TSE imaging took 20 minutes to cover 21-cm-long course of SFA and thus would demand up to 40 minutes to allow for the same coverage as used in SPACE imaging.

DISCUSSION

The present study demonstrates that SPACE technique was able to provide imaging of the SFAs wall with submillimeter, isotropic spatial resolution in a clinically acceptable scan time of 11 minutes. We have found that scan time was reduced, CNR and CNR_{eff} were significantly improved and there was no significant difference in the measurement of morphological characteristics of the vessels wall. We have observed that SPACE images provides images superior to standard 2D TSE T2w images [11].

Conventional multislice 2D saturation-band TSE imaging has become a typical MR technique for assessing arterial wall and atherosclerotic plaques by providing multi-contrast weighted images [21]. Its application, however, is limited by two major shortcomings: 1) relatively low spatial resolution in the slice-select direction due to the poor slice profile of its selective excitation, thus making 2D images more prone to partial volume effect; 2) long acquisition times for achieving sufficient SNR and/or high in-plane spatial resolution. In comparison, 3D acquisition is advantageous because of both intrinsic high SNR, which may be traded for high spatial resolution, and potentially improved voxel isotropy and anatomic coverage. It is also noteworthy that 3D imaging allows for retrospectively visualizing vessel in any orientation through multi-planar reformatting, which is essential for assessing morphology of vessel wall and lumen.

Recently, a 3D balanced steady-state free precession (bSSFP) acquisition combined with a motion-sensitized driven-equilibrium (MSDE) magnetization preparation was used for black-blood arterial wall imaging [19,22]. However, at high field strength such as 3.0T, bSSFP suffers from off-resonance artifacts resulting from main magnetic field inhomogeneity. Another 3D imaging technique, variable flip-angle single-slab 3D TSE with long echo trains (called SPACE in Siemens®, XETA in GE®), has been lately introduced as an alternative for T2w fast imaging of carotid arterial wall at 3.0T showing robust image quality due to its insensitivity to field inhomogeneities [23]. This is the first report of the application of the SPACE technique to the problem of assessing peripheral vascular disease.

Compared with the conventional 3D TSE where high-degree refocusing RF pulses are used, the single-slab 3D TSE technique employs variable low-flip-angle refocusing RF pulses and achieves lower power deposition and a longer echo train with sufficient signal levels that favors fast imaging [14,15,16]. In this sequence, a slab-selective excitation (90°) and the first spatially

nonselective refocusing (180°) RF pulses are followed by a series of variable low-flip-angle refocusing pulses.

The flip-angle series is prospectively configured based on a tissue-specific prescribed signal evolution that usually undergoes three phases successively (for example, a brief signal decay in the first few echoes followed by a pseudo-steady-state (PSS) that yields a relatively constant signal level over most part of the echo train, and finally a second exponential signal decay).

It is known that 3D TSE acquisition has inherent black-blood effect based on motion-induced intravoxel dephasing [24]. In the SPACE, this effect is enhanced by the use of lower refocusing flip-angles and long echo trains that induce larger phase dispersion, especially when flow direction is along the readout axis [25]. Chung et al. has demonstrated that this technique is capable of providing black-blood T2-weighted images of carotid arterial walls that were comparable to those obtained using conventional 2D TSE [23].

In most studies published to date validating 2D TSE MR imaging in humans, findings were obtained in the carotid arteries and several studies evaluated atherosclerotic plaque progression in humans, but few studies have evaluated the utility of MRI in measuring signal intensity and morphology in the peripheral circulation. Recently, a study reported that multislice 2D saturation-band TSE with high resolution ($0.5 \times 0.5 \times 3$ mm^3, voxel volume 0.75 mm^3) measured plaque volume in PAD is reliable and reproducible at 1.5 T MR System [11]. It required long imaging time to cover the entire SFAs (40 minutes) with multiple measurements, resulting in relatively low CNR efficiency. In another study, 7 patients with PAD were examined by both MRI and intravascular ultrasound and 3D TOF sequence was used to measure vessel wall parameters with an in-plane resolution of $0.78 \times 0.49 \times 2$ mm^3 and an image voxel volume of 0.76 mm^3 [12]. This bright blood technique consistently overestimates plaque area compare to dark blood TSE sequences. Song et al and Parker et al proposed time efficient 2D DIR-prepared fast SE sequences that allow data acquisition of multiple sections (up to four) within one repetition time [26]. DIR technique is more effective in suppressing blood signals compared to spatial saturation bands in the case of single-slice or thin-slab multi-slice 2D imaging. However, a previous study has shown that, when thick-slab (about 12 slices × 3.3 mm) multi-slice 2D imaging is performed, these two techniques yield no significant difference in lumen SNR and wall-lumen CNR [17]. The investigators also demonstrated that the vessel wall area and lumen area were not affected using the 2D DIR or blood flow saturation band sequences [17]. Thus, 2D TSE sequence with flow saturation bands was applied to generate BB for comparison with 3D SPACE in our study. A 39mm-thick imaging slab was employed, which is similar to the thickness used in Mani et al [17]. We acknowledge that in-flow of inverted blood spins may not be sufficient with this thickness value and may compromise the quality of black-blood effect within the slices at flow downstream. It is a common issue for this kind of in-flow dependent techniques that a trade-off is required between black suppression and time efficiency (coverage).

The SFA represents an interesting vascular region for high resolution MR imaging examinations of vessel wall and atherosclerotic plaque changes. It is true that imaging SFAs dose not involve artifacts resulting from heart beat, respiration, or swallowing, but there are other sources of motion artifact for SFA that can be difficult or impossible to overcome such as involuntary twitching which can not be eliminated by coaching or cajoling the patient. In addition, the position of the SFA permits the use of commercial surface coils with the associated high signal efficiency. The MR imaging protocol presented in our study allowed for the precise correlation of 3D imaging slices to the corresponding position of 2D imaging slices. It is needed to develop an approach to high isotropic resolution assessment of vessel wall and lumen in the peripheral circulation with mild to moderate PAD. In our study, SPACE provided high isotropic resolution ($0.72 \times 0.72 \times 0.72$ mm^3, voxel volume is 0.52 mm^3) with high CNR efficiency and

significant improvement of imaging speed. The SPACE pulse sequence offers a few important advantages and the results showed that 3D vessel wall imaging of the SFA with the SPACE technique is feasible. First, we compared 3D SPACE imaging with conventional 2D TSE T2w imaging in the quantification of SFA vessel wall and lumen. The results from the present study indicated SPACE imaging's capability to measure vessel wall and lumen parameters and reliably quantify vessel wall, which were in excellent agreement with those measured by conventional 2D TSE T2w technique. With submillimeter, $0.72 \times 0.72 \times 0.72$ mm^3 isotropic resolution (image voxel volume 0.37 mm^3), potential applications of 3D SPACE include diagnosing preclinical vascular disease, assessing disease severity in those with established PAD, and monitor atherosclerotic plaque progression. Future study is needed to assess the utility of 3D SPACE in monitoring atherosclerotic disease.

A second advantage of SPACE is its capability to reformat images into arbitrary planes. With the aid of MPR, sections of the vessels on multiple orientations were shown, not limited to the axial plane, but also showed any orientation of the vessel wall. This is particularly true along the vessel long axis, which provides an overview of wall morphology (figure 3). SPACE imaging provides the potential application to assess the important aspects of SFA lesions, such as their extension along the vessel, cross-sectional appearance, and composition with high isotropic resolution. For the purpose of assessing plaque composition, the 3D SPACE sequence may need to be configured into different versions capable of T1, T2, and proton-density weighting contrasts, and also possibly be used in combination with TOF. Also, images obtained by MPR will permit the measurement of the obstruction caused by an atherosclerotic lesion, as true cross-sectional views of the stenotic site can be obtained in a clinical setting. On the other hand, compared with images acquired directly in reconstruction plane with 2D TSE, the reformatted SPACE images were similar in depiction of anatomy, with much thinner slices. Reformations in multiple planes could increase the time required to examine the images, although images could be reformatted automatically in the reconstruction or in post-processing before being presented to the radiologist. Reformations of the 2D FSE images are not routinely obtained owing to the relatively thick slices with interslice gaps. Third, SPACE allowed imaging at a faster speed than did 2D saturation band TSE sequence (3D vs. 2D, 11.4 vs. 40 minutes) and large coverage to be achieved in a time-efficient way and with good image quality. It is a time-efficient method to enable SFA wall imaging at clinical setting. It is notewothy that the achieved time efficiency was associated with a large longitudinal coverage of 380 mm in this study, which favored the CNR comparison. This high CNR efficiency could not hold true in other vascular territories where a long coverage is not needed. However, the capability of 3D SPACE for characterizing arterial wall or plaque composition needs further investigation.

The use of fat suppression with 3D SPACE does not change the imaging time for this sequence or affect the anatomic coverage of SFA. This is because the majority of time within one TR is for signal recovery rather than acquiring data from adjacent slices. In multi-slice 2D TSE, fat saturation module is applied prior to image acquisition of each slice, taking a period of 17 msec each time. This would limit the number of slices to be acquired with TR being fixed.

This study shows the potential for using SPACE in normal volunteers. Future studies are required to show the diagnostic accuracy of SPACE compared with routine sequences for the patients with PAD. Reduced blood flow present in patients may lead to incomplete flow suppression, thereby compromising black-blood effect in SPACE imaging. The imaging time with SPACE is still long that may not be tolerated by some patients. More efforts, such as parallel imaging in both phase-encoding and partition-encoding, could be made to accelerate the scans.

In conclusion, SPACE is a fast MR imaging sequence that enables black-blood superficial femoral arterial wall imaging with an adequate spatial coverage, isotropic high spatial

resolution, and superior CNR and time efficiency. The isotropic-resolution SPACE images, with the aid of MPR, allows for imaging vessel wall in any orientation without signal loss which is not possible with 2D TSE. This is particularly helpful along the vessel long axis that provides an overview of vessel wall morphology. Furthermore, the ability to view images at arbitrary slice thicknesses and in oblique and curved planes may improve depiction of anatomy and diagnosis of abnormality.

REFERENCES

1. Rosamond W, Flegal K, Friday G, Furie K, Go A, Greenlund K, Haase N, Ho M, Howard V, Kissela B, Kittner S, Lloyd-Jones D, McDermott M, Meigs J, Moy C, Nichol G, O'Donnell CJ, Roger V, Rumsfeld J, Sorlie P, Steinberger J, Thom T, Wasserthiel-Smoller S, Hong Y, American Heart Association Statistics Committee and Stroke Statistics Subcommittee. Heart disease and stroke statistics--2007 update: a report from the American Heart Association Statistics Committee and Stroke Statistics Subcommittee. Circulation 2007;115(5):e69–171. [PubMed: 17194875]
2. Makowsky MJ, McAlister FA, Galbraith PD, Southern DA, Ghali WA, Knudtson ML, Tsuyuki RT, Alberta Provincial Program for Outcome Assessment in Coronary Heart Disease (APPROACH) Investigators. Lower extremity peripheral arterial disease in individuals with coronary artery disease: prognostic importance, care gaps, and impact of therapy. Am Heart J 2008;155(2):348–355. [PubMed: 18215607]
3. Hirsch A, Haskal Z, Hertzer N, et al. ACC/AHA guidelines for the management of patients with peripheral arterial disease (lower extremity, renal, mesenteric, and abdominal aortic): executive summary: a collaborative report from the American Association for Vascular Surgery/Society for Vascular Surgery, Society for Vascular Medicine and Biology, Society of Interventional Radiology, and the ACC/AHA Task Force on Practice Guidelines (Writing Committee to Develop Guidelines for the Management of Patients With Peripheral Arterial Disease [Lower Extremity, Renal, Mesenteric, and Abdominal Aortic]). J Am Coll Cardiol 2006;47:e1–e192. [PubMed: 16386656]
4. Abramson BL, Huckell V, Anand S, et al. Canadian Cardiovascular Society Consensus Conference: peripheral arterial disease—executive summary. Can J Cardiol 2005;21:997–1006. [PubMed: 16234879]
5. McDermott MM, Mehta S, Ahn H, et al. Atherosclerotic risk factors are less intensively treated in patients with peripheral arterial disease than in patients with coronary artery disease. J Gen Intern Med 1997;12:209–215. [PubMed: 9127224]
6. Halliburton SS, Schoenhagen P, Nair A, Stillman A, Lieber M, Murat Tuzcu E, Geoffrey Vince D, White RD. Contrast enhancement of coronary atherosclerotic plaque: a high-resolution, multidetector-row computed tomography study of pressure-perfused, human exvivo coronary arteries. Coron Artery Dis Sep;2006 17(6):553–60. [PubMed: 16905968]
7. Worthley SG, Helft G, Fuster V, Fayad ZA, Fallon JT, Osende JI, Roqué M, Shinnar M, Zaman AG, Rodriguez OJ, Verhallen P, Badimon JJ. High resolution ex vivo magnetic resonance imaging of in situ coronary and aortic atherosclerotic plaque in a porcine model. Atherosclerosis Jun;2000 150(2): 321–9. [PubMed: 10856524]
8. Yuan C, Kerwin WS, Yarnykh VL, Cai J, Saam T, Chu B, Takaya N, Ferguson MS, Underhill H, Xu D, Liu F, Hatsukami TS. MRI of atherosclerosis in clinical trials. NMR Biomed 2006;19(6):636–654. [PubMed: 16986119]
9. Wentzel JJ, Aguiar SH, Fayad ZA. Vascular MRI in the diagnosis and therapy of the high risk atherosclerotic plaque. J Interv Cardiol 2003;16(2):129–42. [PubMed: 12768916]
10. Summers RM, Andrasko-Bourgeois J, Feuerstein IM, Hill SC, Jones EC, Busse MK, Wise B, Bove KE, Rishforth BA, Tucker E, Spray TL, Hoeg JM. Evaluation of the aortic root by MRI: insights from patients with homozygous familial hypercholesterolemia. Circulation 1998;98(6):509–18. [PubMed: 9714107]
11. Isbell DC, Meyer CH, Rogers WJ, Epstein FH, DiMaria JM, Harthun NL, Wang H, Kramer CM. Reproducibility and reliability of atherosclerotic plaque volume measurements in peripheral arterial disease with cardiovascular magnetic resonance. J Cardiovasc Magn Reson 2007;9(1):71–6. [PubMed: 17178683]

12. Meissner OA, Rieger J, Rieber J, Klauss V, Siebert U, Tató F, Pfeifer KJ, Reiser M, Hoffmann U. High-resolution MR imaging of human atherosclerotic femoral arteries in vivo: validation with intravascular ultrasound. J Vasc Interv Radiol Feb;2003 14(2 Pt 1):227–31. [PubMed: 12582191]

13. Chung, Yiu-Cho; Menzel, Marion; Raman, Subha V.; Simonetti, Orlando P. 3D Dark Blood TSE for Carotid Vessel Wall Imaging. Proc 14th ISMRM 2006:653.

14. Mugler, John P.; Keifer, Robert B.; Brookeman, James R. Three-dimensional T2-weighted imaging of the brain using very long spin-echo trains. Proc 8th ISMRM. 2000

15. Mugler, John P.; Wald, Lawrence L.; Brookeman, James R. T2-weighted 3D spin-echo train imaging of the brain at 3 Tesla: reduced power deposition using low flip-angle refocusing RF pulses. Proc 8th ISMRM. 2001

16. Busse RF, Hariharan H, Vu A, Brittain JH. Fast spin echo sequences with very long echo trains: design of variable refocusing flip angle schedules and generation of clinical T2 contrast. Magn Reson Med 2006;55(5):1030–7. [PubMed: 16598719]

17. Mani V, Itskovich VV, Aguiar SH, Mizsei G, Aguinaldo JG, Samber DD, Macaluso FM, Fayad ZA. Comparison of gated and non-gated fast multislice black-blood carotid imaging using rapid extended coverage and inflow/outflow saturation techniques. J Magn Reson Imaging 2005;22(5):628–33. [PubMed: 16215965]

18. Isoda H, Kataoka M, Maetani Y, Kido A, Umeoka S, Tamai K, Koyama T, Nakamoto Y, Miki Y, Saga T, Togashi K. MRCP imaging at 3.0 T vs. 1.5 T: preliminary experience in healthy volunteers. J Magn Reson Imaging 2007;25(5):1000–1006. [PubMed: 17410562]

19. Koktzoglou I, Li D. Diffusion-prepared segmented steady-state free precession: Application to 3D black-blood cardiovascular magnetic resonance of the thoracic aorta and carotid artery walls. J Cardiovasc Magn Reson 2007;9(1):33–42. [PubMed: 17178678]

20. Alizadeh Dehnavi R, Doornbos J, Tamsma JT, Stuber M, Putter H, van der Geest RJ, Lamb HJ, de Roos A. Assessment of the carotid artery by MRI at 3T: a study on reproducibility. J Magn Reson Imaging 2007;25(5):1035–43. [PubMed: 17457802]

21. Yuan C, Mitsumori LM, Beach KW, Maravilla KR. Carotid atherosclerotic plaque: noninvasive MR characterization and identification of vulnerable lesions. Radiology 2001;221(2):285–299. [PubMed: 11687667]

22. Koktzoglou I, Li D. Submillimeter isotropic resolution carotid wall MRI with swallowing compensation: imaging results and semiautomated wall morphometry. J Magn Reson Imaging 2007;25(4):815–823. [PubMed: 17345637]

23. Chung, Yiu-Cho; Du, Jianjun; Weale, Peter; Sheehan, John; Carr, James; Zhang, Qiang; Jerecic, Renate. Carotid Artery Imaging at 3T: More Signal from 3D Imaging Using a New 4-Element Coil. Proc 15th ISMRM. 2007

24. Alexander AL, Buswell HR, Sun Y, Chapman BE, Tsuruda JS, Parker DL. Intracranial black-blood MR angiography with high-resolution 3D fast spin echo. Magn Reson Med 1998;40(2):298–310. [PubMed: 9702712]

25. Mugler, John P. Motion-artifact-free T2-weighted 3D imaging of the cervical spine. Proc 8th ISMRM. 2000

26. Song HK, Wright AC, Wolf RL, Wehrli FW. Multislice double inversion pulse sequence for efficient black-blood MRI. Magn Reson Med 2002;47(3):616–620. [PubMed: 11870851]

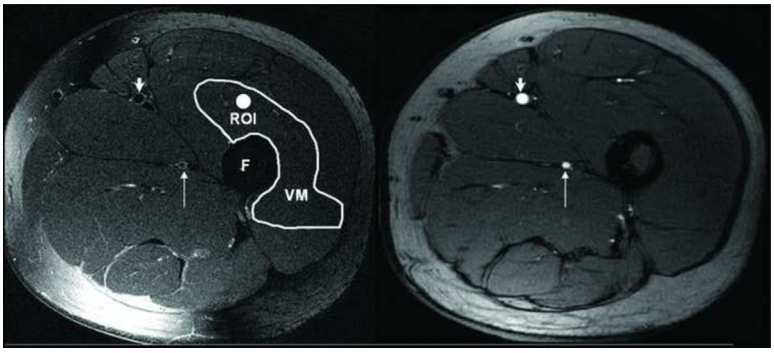

Figure1.

Matched two axial cross-sectional images of left SFA in 34-year-old woman, left one is 2D T2w TSE image, right one is the same location slice, but the image from 2D TOF scout. SFA are pointed by short arrows on the two images, long arrows point deep femoral artery. TOF image in the two arteries is consistent with 2D T2W TSE image. Note the similarity in size and shape of the SFA and deep femoral artery on both images. An ROI for signal and noise measurements are depicted as a bright circle in the vastus medialis muscle (VM) on the left image. F is femur.

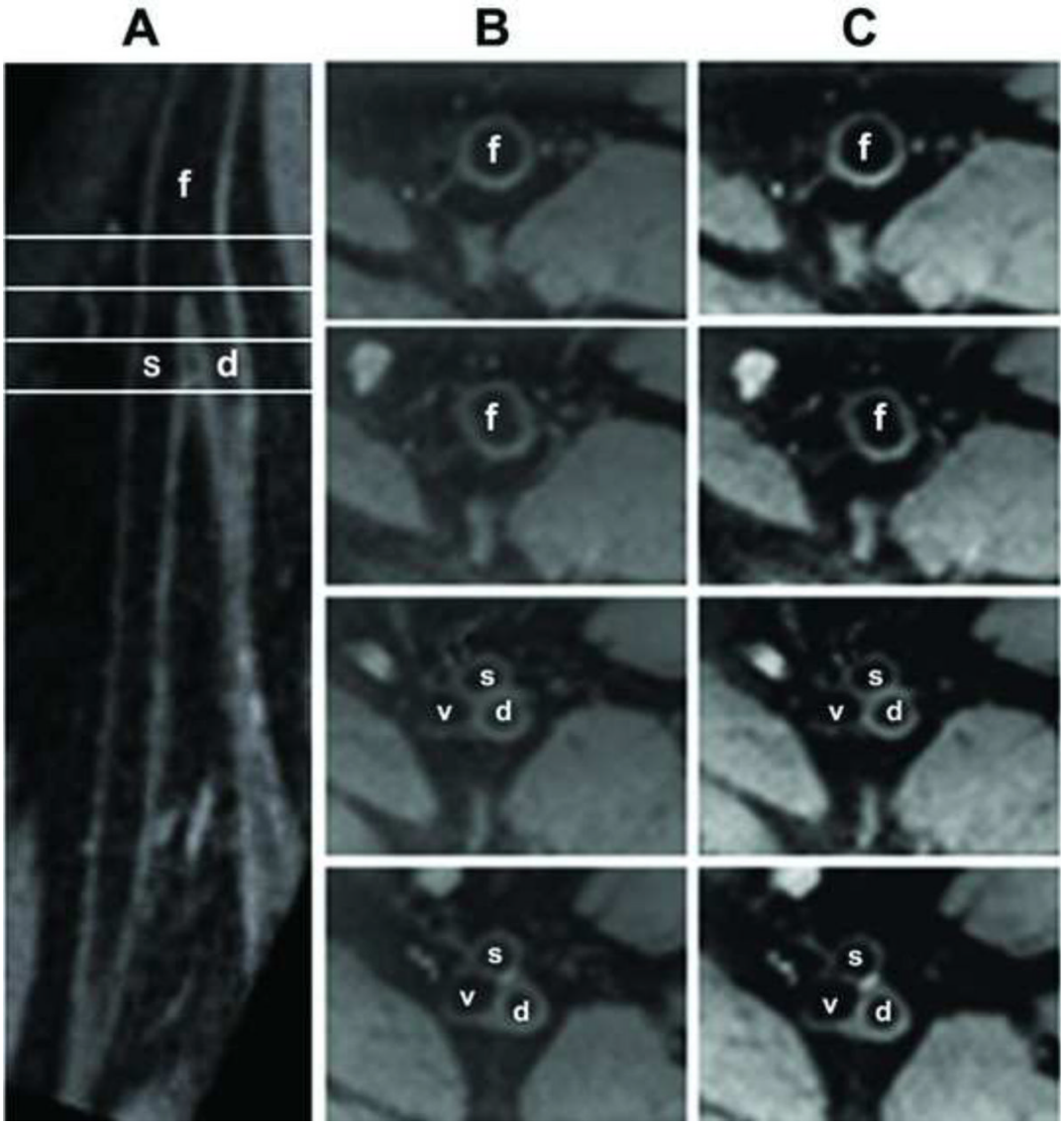

Figure 2.
Typical images from healthy volunteer, male, 34 years old: Panel A is curved MPR (slice thickness = 3 mm) reconstructed from 3D SPACE data set showing the femoral bifurcation (into superficial and deep femoral arteries) with very clear vessel wall and lumen delineation. Panel B shows four slices of 2D T2w TSE axial images corresponding to the line marks on panel A (up to down: common femoral artery, right above bifurcation, bifurcation and SFA/deep femoral artery sections), and panel C is the pair of 2D cross-sectional images (slice thickness = 3 mm) of SFA were reconstructed from 3D SPACE data by MPR, f: common femoral artery, s: SFA, d: deep femoral artery, v: femoral vein.

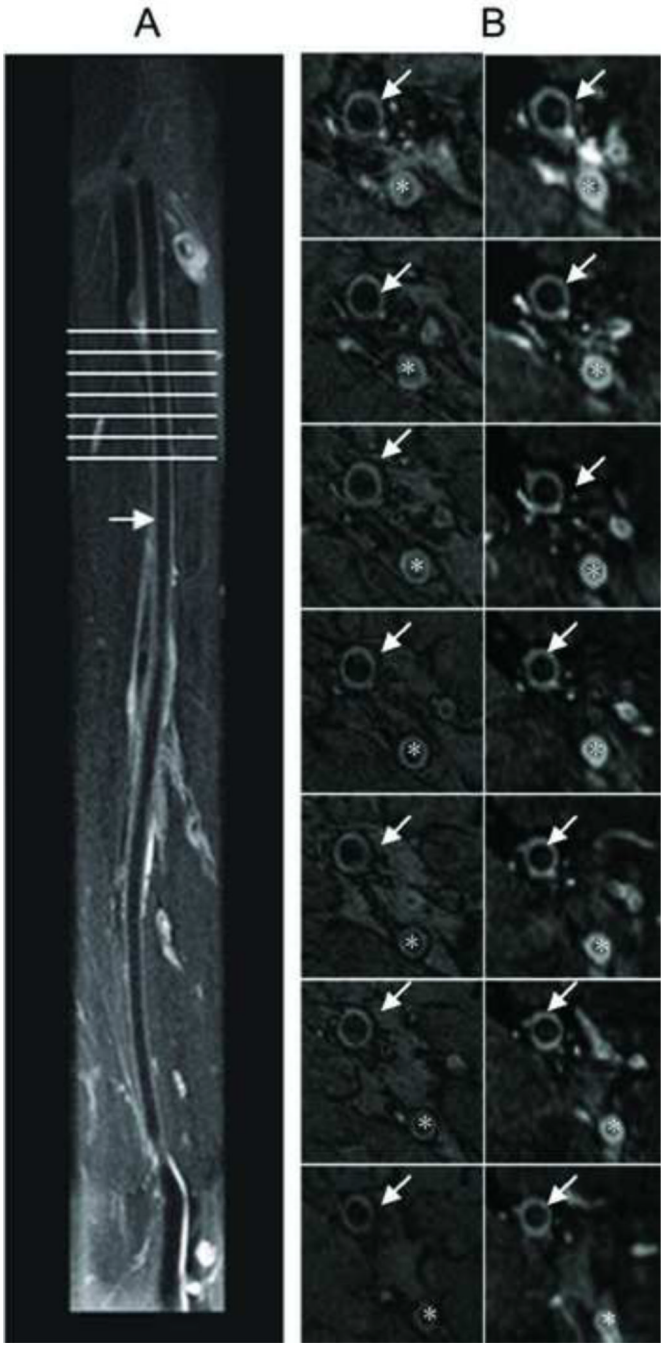

Figure 3.
Typical SFA SPACE results: the volunteer is 32 years old, man; Curved MPR image (slice thickness = 3 mm) shows the longitudinal view of SFA acquired using SPACE on panel A. Panel B (left) shows 7 axial slices of 2D T2w TSE images of SFA from line mark on panel A, Panel B (right), the pairs of 3D SPACE cross-sectional images of the arterial wall created by MPR. Imaging time is 11.32 minutes with 38 cm coverage of bilateral SFAs, arrow points SFA, * deep femoral artery.

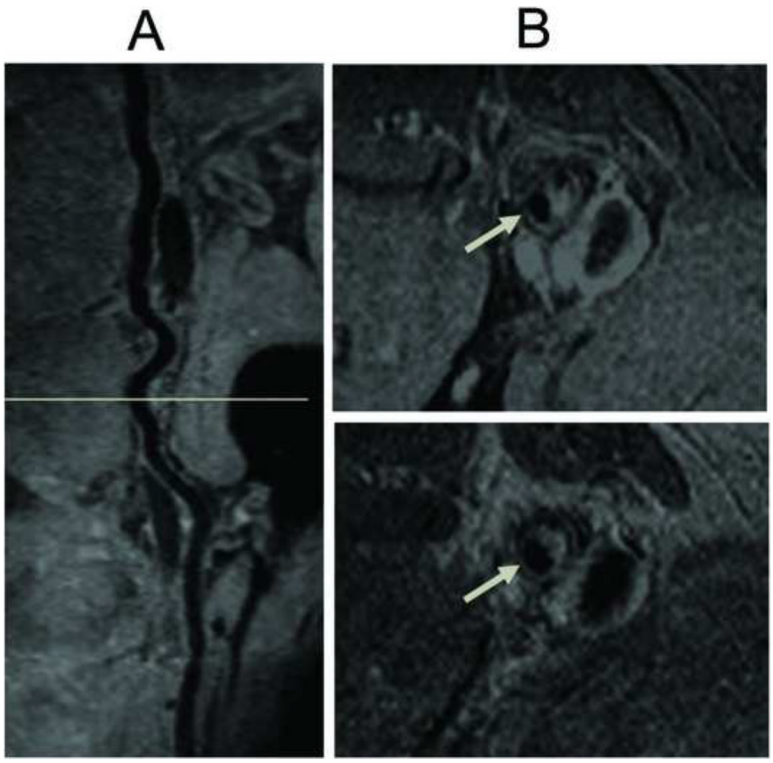

Figure 4.
Typical SFA SPACE results: the PAD patient is 72-year-old male with ABI of 0.6. MPR of SPACE shows a longitudinal view of SFA with extensive plaques in panel A. Panel B, cross-sectional MPR image with 3mm slice thickness of SPACE images on top (from the plane marked in panel A). On the bottom of panel B is the corresponding 2D TSE T2w image, respectively. Each of these cross-section images shows the atherosclerotic plaques (arrow).

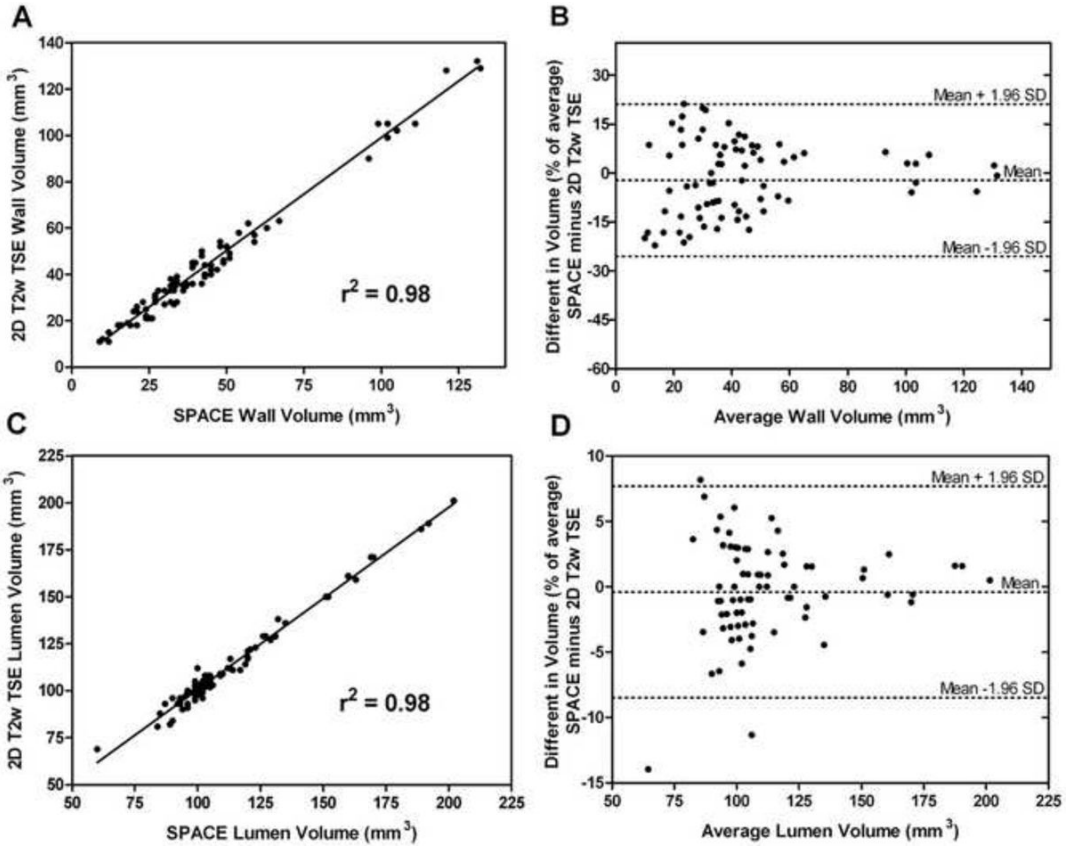

Figure 5.

Panel A: Scatter plot of SFA WV as measured from the 3D SPACE and 2D TSE T2W images. Panel B: Bland-Altman plot of percentage difference in SFA WV versus average SFA WV showing the limits of agreement. Panel C: Scatter plot of SFA LV as measured from both sequences. Panel D: Bland-Altman plot of percentage difference in SFA LV versus average SFA LV showing the limits of agreement.